Matematisk-fysiske Meddelelser
udgivet af
Det Kongelige Danske Videnskabernes Selskab
Bind **35,** nr. 4

Mat. Fys. Medd. Dan. Vid. Selsk. **35,** no. 4 (1966)

STOPPING POWER OF ALUMINIUM FOR 5-12 MeV PROTONS AND DEUTERONS

BY

H. H. ANDERSEN, A. F. GARFINKEL,
C. C. HANKE, AND H. SØRENSEN

København 1966
Kommissionær: Munksgaard

CONTENTS

Synopsis

The stopping power of aluminium for 5–12 MeV protons and deuterons has been measured by a thermometric compensation technique working at liquid helium temperature. The experimental method is described and the standard deviation of the results is found to be 0.3 %. In order to obtain this accuracy one has to apply theoretical corrections for the influence of Coulomb scattering, x-rays and δ-rays. Other possible corrections are discussed, but are found to be negligible for this combination of projectiles, energies and target material. The results agree with published experimental results as well as with Bichsel's semiempirical tables.

PRINTED IN DENMARK
BIANCO LUNOS BOGTRYKKERI A/S

I. Introduction

The measurement of energy losses and ranges of protons and deuterons is an old topic in atomic physics, and a vast amount of data has been collected during the years. BICHSEL has recently tried to present a detailed comparison between experimental material and theory (BICHSEL 1961, 1963, 1964). It turned out, however, that the accuracy of the existing data was not high enough to yield unambigous results for the so-called "shell-corrections" and there is thus a need for more accurate data. Until now methods utilizing nuclear instrumentation have been used and the best results obtained was 0.5 % for range (BICHSEL et al. 1957, BICHSEL 1958) and 1–2 % for stopping power measurements (NIELSEN 1961). To obtain more accurate results it is either necessary to build expensive energy analysing systems or to use new principles. The latter has, e.g., been tried by KALIL et al. (1959) and ZIEMER et al. (1959) who measured energy losses in thin foils directly by calorimetric methods. The accuracies obtained could compete with those of conventional techniques only in the special case of very low energy electrons. The idea to make a direct measurement of the energy loss has also been used in the present investigation. Our method utilizes a thermometric compensation technique working at liquid helium temperature, and avoids the conflict between target size and resolution of the analysing system. It is thus possible to measure stopping powers of thin metal foils accurately in spite of unavoidable inhomogenities in foil thicknesses.

The measurements were done at the tandem van de Graff laboratory of the Niels Bohr Institute, the University of Copenhagen. The projectiles were 5–12 MeV protons and deuterons. As a target aluminium was first chosen since this material has often been used as a sort of standard for relative stopping power measurements.

II. Experimental Procedure

A. Energy Losses

A determination of stopping power from a measurement on a thin foil requires a determination of three different quantities: the energy of the incoming particle, the energy loss in the foil, and the thickness of the foil. Since the measurement of energy and foil thickness only involves standard techniques we will first discuss the measurement of the energy loss.

The principle is shown in fig. 1. The target foil and a block thicker than the range of the projectiles are connected to a heat sink through thermal resistances W_F and W_B. The beam passes through the foil and is stopped in the block. It causes a heating of foil and block giving temperature rises measured with the thermometers R_F and R_B. The beam is then switched off, and electrical powers P_F and P_B are fed to heaters thermally connected to foil and block until the same temperature rises are obtained. A particle having energy E_0 immediately in front of the foil will suffer an energy loss ΔE in the foil given by the relation

$$\Delta E = E_0 \frac{P_F}{P_F + P_B}. \tag{2.1}$$

The requirement for obtaining a good determination of the above power ratio is that the conditions corresponding to heating by the beam are well reproduced by the electrical heaters. This is fulfilled if both systems, foil and block, are isolated to the extent that they can only interact thermally with the heat sink, and that these interactions only take place through their thermal resistances. Especially should there be no mutual thermal interaction between block and foil.

The actual experiment is performed with a liquid helium bath as heat sink. The system is placed in vacuum and surrounded by a thermal shield at liquid helium temperature. The low temperature guaranties that interactions by thermal radiation will be very small, and it is also easy to obtain such a good vacuum that heat transfer through the residual gas is negligible. Furthermore, the absolute sensitivity of thermometers is greater at lower temperatures so that a smaller temperature rise is necessary to obtain a given accuracy. This factor, small temperature rises, also reduces the radiation interactions. Finally, in order to make the system able to respond quickly to changes in beam current or electrical power, the thermal time constants of the two systems should be small. This is most easily obtained

at low temperatures, where heat capacities are small and thermal conductivities high.

If the foil itself has poor heat conductivity, the center of the spot hit by the beam may become very hot, and thermal radiation will be important. Both to avoid this, and to keep the thermal time constants low, it is necessary to work with targets having good heat conductivity at liquid helium temper-

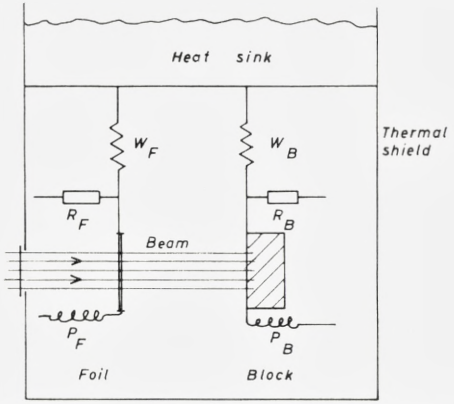

Figure 1. Diagram of stopping power measuring system. W_F and W_B are thermal resistances, R_F and R_B thermometers, and P_F and P_B electrical heaters.

atures. This means that the method is only applicable to pure metals in its present form.

The measurements are made using a commercial liquid helium irradiation cryostat (Hofmann Inc.). The measuring equipment is fastened to the bottom of the cryostat as shown in fig. 2. The helium cryostat is cut open, and the radiation shields at liquid nitrogen and liquid helium temperature (77°K and 4.2°K) are not shown. Beneath the cryostat the target foil is seen. It is soldered to a frame of well annealed very pure copper, and the heater is wound around the frame near the soldering point. The frame is mechanically fastened to the cryostat by insulating pins, and the heat path is provided by a copper wire. The length and thickness of the copper wire, and thus the thermal resistance, may easily be varied. The thermometer is an ordinary 0.1 Watt carbon resistor. The resistance of the thermometer is 68 Ω at room temperature, 290 Ω at 10°K and 850 Ω at 4.2°K, giving enormous sensitivity in the lower temperature range. The thermometer is fastened near the end of the thermal resistance.

The stopping block is shown behind the foil. It is an aluminium case

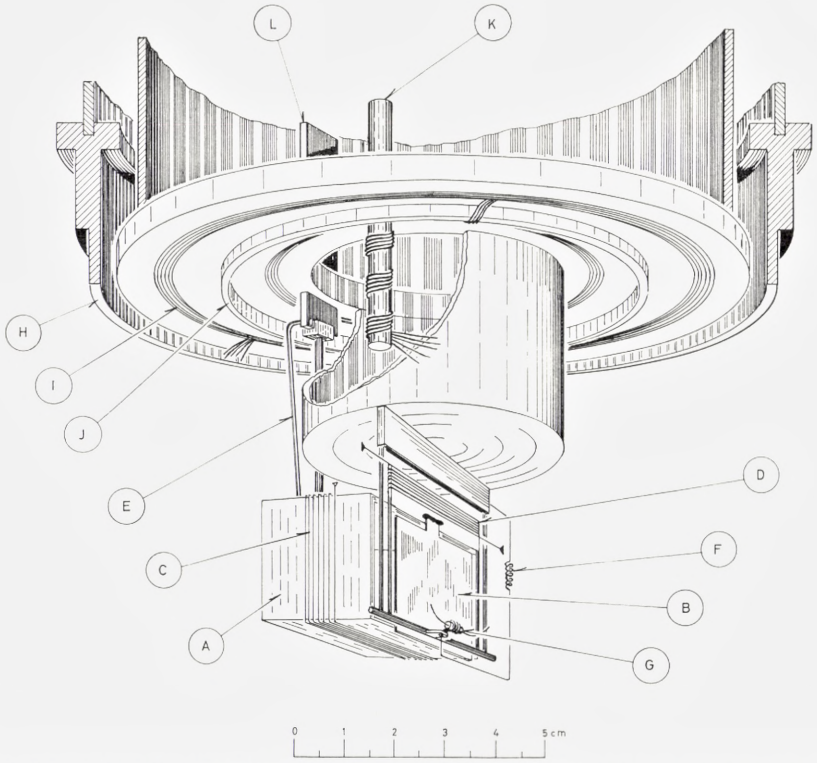

Figure 2. The set-up for stopping power measurements, showing the lower part of the helium Dewar (cut open), the measuring equipment, and the nitrogen temperature shield. A. Stopping block. B. Target foil. C. and D. Heaters. E. and F. Heat paths with resistances. G. Foil thermometer. H. Nitrogen temperature shield. I. Electrical connections laquered to the bottom of the helium Dewar. J. Copper edge to which helium temperature radiation shield is fastened. K. and L. Thermal connections to helium bath. Note that the electrical connections from the bottom of the Dewar to block and foil are not shown.

open in the side facing the foil. The opposite side, where the beam is stopped, is made from a 0.3 mm gold plate, this particular metal being chosen to reduce the influence of nuclear reactions. This shape has been chosen partly to ensure that particles have to be Coulomb scattered in the foil by more than $\pi/2$ to avoid hitting the block, and partly to ensure that most x-rays emitted from the gold surface are reabsorbed by the block and not by the foil. Heater, thermal resistance, and thermometer are placed in ways similar to those on the foil. The electrical connections to both heaters are made by superconducting Nb_3Zr wire, which has small thermal conductivity. Further details of the construction are given by ANDERSEN (1965) where the characteristics of the system are also discussed.

The usable temperature range is determined by the thermometers. Their sensivity drops off nearly exponentially with increasing temperature, which means that the temperature increase should be kept reasonably low. We also need a fairly big temperature increase to be able to measure it accurately. These competing factors give the sensitivity of the system a broad maximum between 6 and 10°K. The temperature rise of each system can then be varied a factor of three without affecting the accuracy, meaning that power ratio variations within a factor of nine are permissible.

It has, until now, been assumed that the intensity of the accelerator beam is stable, and that this defines one temperature rise for each of the systems. This is, unfortunately, not the case. Two temperature intervals rather than two temperatures are thus defined. The calibration with the electrical heaters should cover the same temperature intervals, and three calibration points are made for each system. Large variation in beam current will reduce the accuracy of the measurement and calibration, and variations larger than 10 % are normally not accepted.

The temperatures of block and foil should follow the beam current variations reasonably well, and small time constants are thus very important for the method. The time constants are 3–7 seconds for the foil and 0.5–1.5 seconds for the block, increasing with increasing temperature. This is satisfactory, although a smaller time constant for the foil would be advantageous.

The fluctuating temperatures are measured continuously and simultaneously. This is done with Wheatstone bridges, one for each system, the bridges being set at suitable values in order to give signals varying around zero. The signals are amplified and fed into recorders. It is then possible to select corresponding points on the two recorder curves. The method used for the evaluation of energy losses from recorder readings will be described later.

The determination of the energy loss has been tested in different ways. Two of these tests will be described here. They are both concerned with the problem, whether we really measure all the heat dissipated in the foil and the block. (The problem whether all the dissipated energy appears as heat or not is treated later). The compensation technique may be erroneous either if there are radiation losses or if the heat dissipated by the beam does not choose the same heat paths to reach the reservoir as that supplied by the heaters. If either of these is the case, measurements with different beam intensities will yield different results. This has been tested with 6 MeV protons in aluminium. The result is shown in fig. 3. There is no trend in the results – all agree with each other within 0.1 %.

To check the internal consistency of the calibrations we have done

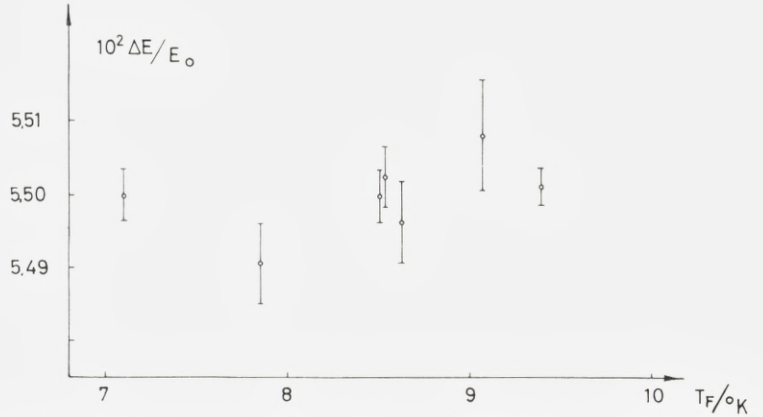

Figure 3. Relative energy loss for 6 MeV protons in an aluminium foil. The beam intensity is varied by a factor of two, and no significant variation with intensity is observed.

measurements with superposed power on the block heater. This test has been done twice with aluminium and twice with copper. When the known power is subtracted afterwards it is possible to evaluate the stopping power. The added power is chosen to have the same magnitude as that provided by the beam. These results, compared with others obtained without superposed power, are given in table 1. Again no trend is seen, and we conclude that we measure the power ratio to within $0.1\,^0/_0$.

TABLE 1. The influence of superposing the beam with power on the block heater.

Target	Proton energy (MeV)	Relative energy loss ($^0/_0$)	
		without overlapping power	with overlapping power
Al	5.001	7.635 ± 0.007	7.648 ± 0.006
Al	5.504	6.421 ± 0.004	6.422 ± 0.003
Cu	6.008	12.435 ± 0.010	12.413 ± 0.011
Cu	6.512	10.763 ± 0.008	10.780 ± 0.008

B. Energy

In the measurements ΔE is obtained from E_0 through (2.1). Stopping power formulas yield roughly $\Delta E \propto 1/E$ (4.2). Thus it is possible and quite convenient in the following graphs and tables of ΔE (or dE/dx) versus

energy to assume the energy to be a precise number and to attribute to ΔE twice the relative uncertainty in the actual measured value of E_0. An uncertainty of $0.1\,\%$ in the energy determination will then give $0.2\,\%$ for our stopping power.

The energy E_0 is determined from the field in a 90° deflection magnet. The calibration tables were prepared for a magnet similar in design to the one being used here, (p, n) threshold reactions being utilized. It was assumed that the energy was known within an accuracy of 10 keV through the whole energy range. This yields a relative accuracy of $0.2\,\%$ at 5 MeV giving an uncertainty in the stopping power of $0.4\,\%$ at that energy. This was considered unsatisfactory compared with the other uncertainties involved in the method, and the following calibration programme was therefore carried out. The particles were elastically back-scattered from a thin, heavy-mass target into a heavy-particle spectrograph. The spectrograph was calibrated using α-particles of known energy. The reproducibility of measurements made with different magnetic fields in the spectrograph indicates that it is possible to bring the uncertainty in the energy calibration down by a factor of two, to $0.1\,\%$, by this procedure. As will be seen below this is still our main source of uncertainty, and improved calibration methods are under investigation.

The energy defined by the analysing magnet is, however, not the energy of the particles hitting the foil. Six meters in front of the cryostat are placed a number of 150 μg/cm^2 gold foils, which may be inserted into the beam. The particles undergo multiple scattering in these foils, and the beam is thus spread out, ensuring a homogeneous irradiation of the target foil. Furthermore, the particles pass through 150 μg/cm^2 gold windows in the nitrogen and helium temperature radiation shields. The energy loss suffered in all foils will never exceeded $0.5\,\%$. The resulting energy degradation may be calculated accurately enough not to affect our accuracy.

Particles scattered from collimator edges will have a lower energy than the rest of the beam and will cause the measured stopping powers to be too high. This possibility was tested by varying the number of multiple scattering foils. Inserting more foils will cause a greater relative number of the particles to hit collimator edges and thus give an apparent rise in stopping power greater than the trivial one caused by the change in mean energy. This anomalous rise had a mean value of $0.05\,\%$ in nine experiments with 10–12 MeV deuterons. In each test a measurement was done with 1, 3 and 4 scattering foils, where 3 or 4 are usually used. It was concluded that this is not an appreciable error source and that the total uncertainty in the energy is the calibration error being $0.1\,\%$.

C. Foil Thickness

When we know the energy loss, the stopping power is given by

$$S(E') = \left(\frac{dE}{dx}\right)_{E=E'} = -\frac{\Delta E}{t} \tag{2.2}$$

where $E'(< E_0)$ is defined in part III, and t is the foil thickness. The thickness is determined in the following way. A piece, 6×13 mm, is cut from the foil with a very accurately machined punching tool. Care is taken to ensure that it is the same part of the foil as that irradiated during the energy loss measurements. The area of this piece, and of the hole left in the foil, is measured in a Zeiss Abbe comparator. The mean value is taken as the area, and half the difference as the uncertainty of the area measurement. The weight of the piece is found with a Cahn electrobalance. The total error in the weight per area determination is estimated to be 0.1–0.15 %. In this way we have determined the mean thickness of the same part of the foil as that over which the mean energy loss was measured. For a completely uniform irradiation of this area thickness inhomogeneities of the foil will have very small influence, and one of the main errors in stopping power experiments is thus eliminated. In practice, the number of scattering foils is chosen so that the intensity is not more than 10 % lower at the edges than at the center. Errors due to inhomogeneities will, nevertheless, at least be reduced by a factor of twenty and are insignificant.

The foil is aligned optically to be perpendicular to the beam direction within 2 degrees. We have checked that the foil does not turn or bend while being cooled. Furthermore, the foils contract during cooling, the change in weight/area being twice the linear thermal expansion between 4.2°K and room temperature. The correction is less than 1 % for most metals. Condensation on the target during the measurement can change the apparent thickness in accelerator experiments, especially with cold targets. In our experiment, condensation is not a serious problem because there exists no direct path from the accelerator to the target, and an eventual condensation will take place on the radiation shields and gold windows rather than on the target. Nevertheless, there is sometimes found a small drift which may be detected over long measuring periods. The drift is attributed to condensation of hydrogen or deuterium originating from the ion source. These particles will not condense on the nitrogen shield and only partially on the helium one. The maximum drift found corresponds to about 10 μg aluminium/cm^2 in 12 hours or about 0.2 μg/cm^2/hour of hydrogen.

III. Data Treatment

As mentioned in section II. A, the raw data consist of the power calibrations and the recorder strips showing the off-balance signals from the Wheatstone bridges. The recordings are scanned by eye to obtain corresponding points for the foil and the block. Usually there are no difficulties, but care must be taken to ensure that the systems are in thermal equilibrium at the chosen points. From these pairs of signals corresponding pairs (R_F, R_B) for the resistance of the thermometers are found, and using the power calibrations the sets of corresponding powers (P_F, P_B) are calculated. Equation (2.1) is utilized to calculate the energy loss for each point evaluated. For each energy 15–20 points are used, and the mean value is found together with the standard deviation. There are, apart from this, some systematic errors involved, since any errors in the calibrations are smoothed out and do not show up fully in the fluctuations. Usually the total standard error is below 0.1 % of the mean value (see fig. 3). The entire procedure is very simple, but the numerical work involved is great and has therefore been coded for the GIER computer at Risø.

Equation (2.2) gives the stopping power $S(E')$, which we attribute to the energy E'. To first order in $\Delta E/E$ we have

$$E' = E_0 - \frac{\Delta E}{2}. \tag{3.1}$$

An expansion of $S(E')$ in powers of $\Delta E/E$ gives a quadratic correction term

$$\frac{S_2}{S} = \frac{\Delta E^2}{12}\left(\frac{S'^2}{S^2} - \frac{S''}{S}\right) \tag{3.2}$$

where $S = S(E')$, $S' = \frac{dS}{dE}$, and $S'' = \frac{d^2S}{dE^2}$ (both at E'). Using the nonrelativistic form of the Bethe formula (4.1) and neglecting shell corrections we find

$$\frac{S_2}{S} = \frac{1}{12}\left(\frac{\Delta E}{E}\right)^2\left(\frac{2 - \ln\frac{2mv^2}{I}}{2\left(\ln\frac{2mv^2}{I}\right)^2}\right) \tag{3.3}$$

where m is the electron mass, v the velocity of the projectile and I the mean ionization potential for the target material (see part IV). As the relative

energy loss never exceeds 20 % this correction is always smaller than 0.05 % and is omitted. These results are not identical with those given by ANDERSEN (1965) (p. 35), the latter being wrong due to a calculation error.

A further assumption entering (2.2) is that the trajectory of the projectile through the target is a straight line perpendicular to the foil. This is not the case. Every particle will be Coulomb-scattered through small angles a number of times (multiple scattering). This broadens the angular distribution of the beam as it penetrates into the foil, and the mean distance the particles travel through the foil is thus slightly greater than the foil thickness. Also a small number of particles will be Coulomb-scattered through wide angles and lose nearly all their energy in the foil. Corrections due to these effects are of minor importance for aluminium except for the very thickest targets used, but the corrections are appreciable for heavy targets. The calculation of the corrections is outlined in appendix A and more detailed calculations have been presented by ANDERSEN (1965).

The characteristic angle which separates the two cases is

$$\Theta_1^2 = Nt\frac{\pi e^4 Z^2}{E^2} \tag{3.4}$$

where N is the concentration of target atoms, e is the electronic charge, and Z the atomic number of the target. The relative correction due to multiple scattering is then (see e.g. BETHE and ASHKIN (1953))

$$\frac{\delta_{\text{m.s.}}}{\Delta E} \simeq \Theta_1^2 \cdot f\left(\frac{Z^{2/3} \cdot A}{t}\right). \tag{3.5}$$

A is the atomic mass of the target and f is a slowly varying function nearly equal to two. The correction is of no importance in aluminium, but will, as an example, be 0.18 % for gold with $t = 20$ mg/cm² and $E' = 5$ MeV.

The single scattering term is of more importance. Again, using Θ_1 (3.4) this contribution is

$$\frac{\delta_{\text{s.s.}}}{\Delta E} = \frac{\Theta_1^2}{4}\left[2 + \ln\frac{8}{\Theta_1^2} + 2\ln\frac{E}{\Delta E}\right]. \tag{3.6}$$

This term will exceed 0.1 % for the thickest Al target used (22 mg/cm²). For the above-mentioned case in gold it will be about 0.3 %. The Coulomb corrections are roughly proportional to t, Z and E^{-2}. If the method is extended to other energy regions than those used here, and if one wants the

same relative energy loss as in the present measurements, the thickness must be changed proportionally to E^2. The importance of Coulomb corrections will thus be roughly the same in all energy regions, but for a fixed foil it will be most important for the lowest energy used.

Also the possible influence of the crystal lattice on the results has to be considered. A number of authors have recently found that the stopping power for high-energy particles is lowered appreciably when they move in open directions of the crystal lattice. (Dearnaley, 1964; Dearnaley and Sattler, 1964, 1965; Erginsoy et al., 1964, and Datz et al., 1965). It may, however, be shown theoretically that this will not influence the stopping power of a polycrystalline sample (Lindhard, 1965). There is still the possibility that our samples, which are cut from rolled foils, have a strong crystalline texture, and that some preferred low-indexed crystalline direction accidentally coincide with the beam direction. Whether this is the case or not may be tested experimentally. The concept involved is the following: If a particle hits the foil in a direction which coincides with a low-indexed direction within a certain critical angle, it will be trapped in regions with lower stopping power than the mean value for the material. These critical angles are, in heavy targets, of the order of 0.1° for the energies involved here. In aluminium they will be appreciably smaller (see Lindhard 1964, 1965). They depend only on the energy and charge of the particle, not on its mass, i.e. they are the same for protons and deuterons having the same energy. The critical angles decrease with increasing energy. The foil is not flat within better than 1°, and the total area of the foil perpendicular to the beam direction within the critical angle will thus also decrease with increasing energy. This decrease goes as E^{-1} for trapping along low-indexed directions (the so-called string effect) and as $E^{-1/2}$ for trapping between planes. As is shown below (5.1), protons and deuterons with the same velocity have the same stopping power in an amorphous material, but the deuterons have, in this case, twice the energy of the protons, and the possible influence of a crystal lattice will thus be smaller for the deuterons. We may now compare the measured stopping powers of protons and deuterons with the same velocity. If the deuteron stopping powers are not higher, the crystal lattice has no measurable influence.

Apart from the corrections discussed previously, which have to be applied for all stopping power experiments, there also occur some corrections which are rather specific for the measuring technique used here. We have, until now, assumed that all energy dissipated by the particles in the foil and the block will appear as heat. There is a number of processes

which can occur so that this assumption is not entirely true. The corrections due to this have been discussed in detail by ANDERSEN (1965). We will here summarize the results. The important steps in the calculation of the significant corrections are given in Appendix B.

A certain part of the energy given to the foil may escape through x-rays. A number of processes are competing. One must first calculate the fraction of the energy loss stored in vacancies in inner electron shells. Some of these vacancies are filled in such a way that the liberated energy appears as an Auger-electron and not as an x-ray quantum. The so-called fluorescence yield is the relative number of vacancies in a given shell filled under emission of x-rays. This yield is very low for low Z and for outer shells. Furthermore some of the x-rays will be reabsorbed in the foil. The product of these factors determines the correction. It is insignificant for light elements, but the corrections may be as high as $0.4\,\%$ for thin targets of heavy elements. The evaluation is summarized in Appendix B.

Furthermore, nuclear reactions in the foil and the block will give errors. They are insignificant in our energy range. If we assume the cross-sections to stay roughly constant when the projectile energy is high enough to penetrate the Coulomb barrier, the contribution from these processes will be proportional to the foil thickness and to the particle range in the block. As the range is approximately proportional to E^2, the contribution from nuclear reactions in the block will also increase in proportion to E^2. The errors introduced may be calculated for some elements, but will in all cases be a significant and not too well known correction at high energies.

The usual secondary electron spectrum will have a vanishing influence, but some electrons might get high energies (δ-rays) and introduce an error. It is a surface effect and nearly proportional to E'. (For details see Appendix B). When the proton energy varies from 5 to 12 MeV, the error in the measured energy loss will vary from 500 to 1000 eV. For thin foils and high energies the relative correction will be as high as $0.5\,\%$. The variation with Z is small. Assuming the usual variation of foil thickness for other energy ranges, the importance will decrease as we go to higher energy ranges.

Finally, we have considered the problems of sputtering of foil atoms and of energy stored in point defects in the block. Both are related to the elastic energy transfer to target atoms and are negligible. The effect might be of importance at lower energies.

IV. Outline of Theory

We will give a compressed summary of the theory for stopping power in the energy region of interest here. We are primarily interested in using the theory to find a convenient way of presenting our measured data. An up-to-date review of the present state of the theory has been given by FANO (1963). The theory originating from BETHE yields

$$-\frac{dE}{dx} = \frac{4\pi e^4 z^2}{mc^2\beta^2}\frac{N_0 Z}{A}\left[\ln\left(\frac{2mc^2\beta^2}{1-\beta^2}\right) - \beta^2 - \ln I - \frac{\Sigma C_i}{Z}\right] \tag{4.1}$$

where x is the foil thickness measured in grams/cm^2, N_0 is Avogadro's number, and A is the atomic weight of stopping material in grams. z is the charge of the projectile with velocity $v = \beta c$, Z is the atomic number of the target, and I its mean ionization potential. C_i represents the so-called shell corrections. They are deviations from the simple theory and have been evaluated for the K- and the L-shell by WALSKE (1952 and 1956). The main theoretical interest lies in the calculation of the inner shell corrections from the measurements, their comparison to the WALSKE theory, and the possible experimental evaluation of outer shell corrections for which no theoretical predictions exist.

We see from (4.1) that for a given combination of projectile and target we may write

$$-\frac{dE}{dx} = \frac{a}{E}\ln\frac{E}{b} \tag{4.2}$$

where a and b are energy-independent constants and shell corrections and relativistic effects are neglected. We see then that variation of the energy by a factor of two will also cause dE/dx to vary nearly by the same factor. It is thus not possible to represent our dE/dx-values for the whole energy range in a plot, where we at the same time may see the fluctuations. The most obvious thing to do would be to plot $E \cdot dE/dx$ rather than dE/dx, but this is still not sufficient. We have therefore chosen to use the reduced variable given by BICHSEL (1964). If we define

$$K(\beta) = 4\pi e^4 N_0/mc^2\beta^2 \tag{4.3}$$

and

$$f(\beta) = \ln(2mc^2\beta^2/(1-\beta^2)) - \beta^2 \tag{4.4}$$

we will compute

$$X = f(\beta) + \frac{A}{ZK(\beta)} \left(\frac{dE}{dx} \right)_{\text{exp}} . \tag{4.5}$$

This is in fact an experimental determination of $\ln I + \Sigma C_i/Z$ in eq. (4.1). Theoretically, the shell corrections are found to be positive in our energy range. At very high energies they are zero, and X will then be energy independent and equal to $\ln I$.

V. Results and Discussion

Results will be presented here for measurements with 5–12 MeV protons and deuterons in aluminium. The samples were cut from rolled foils supplied by the United Mineral and Chemical Co., Inc. The purity of the samples as stated by this company was 99.999 %. No corrections for impurities were thus necessary. Measurements have been made on samples with approximate thicknesses of 6, 11, and 22 mg/cm². The thinnest sample is thick enough that no correction is necessary for the unavoidable oxide layer on the aluminium surfaces. The relative energy loss varied from 2 % at high energies in thin foils to 16 % at low energies in thick foils.

The results are presented in fig. 4 in the X-variable defined by eq. (4.5). Note that dE/dx is negative. Thus higher values of X mean numerically lower values for the stopping power. At both ends of the figure is indicated the change, a 1 % change in dE/dx would give in X at that energy. Both proton and deuteron measurements are shown in the reduced energy scale $E \cdot M_p/M$, where M is the mass of the projectile and M_p the proton mass. The deuteron values are therefore indicated at the energy which a proton would have if its velocity were equal to that of the deuteron. The figure contains points measured over a long period of time. During this time significant changes occurred in the energy calibration of the accelerator, and the scatter in the points will therefore reflect the total uncertainty for each point including the calibration uncertainty in E_0. A smooth curve has been fitted by eye through the measured points. The values defined by this curve are listed in table 2. Combination of the errors listed in the preceeding paragraphs yields a total standard deviation in the tabulated values of 0.3 %. As judged from fig. 4 this does not seem to be too optimistic.

It is seen that the proton and deuteron points do not fall together as theory predicts that they should (part IV); we must, however, remember that the proton and the deuteron energy calibrations are made independently

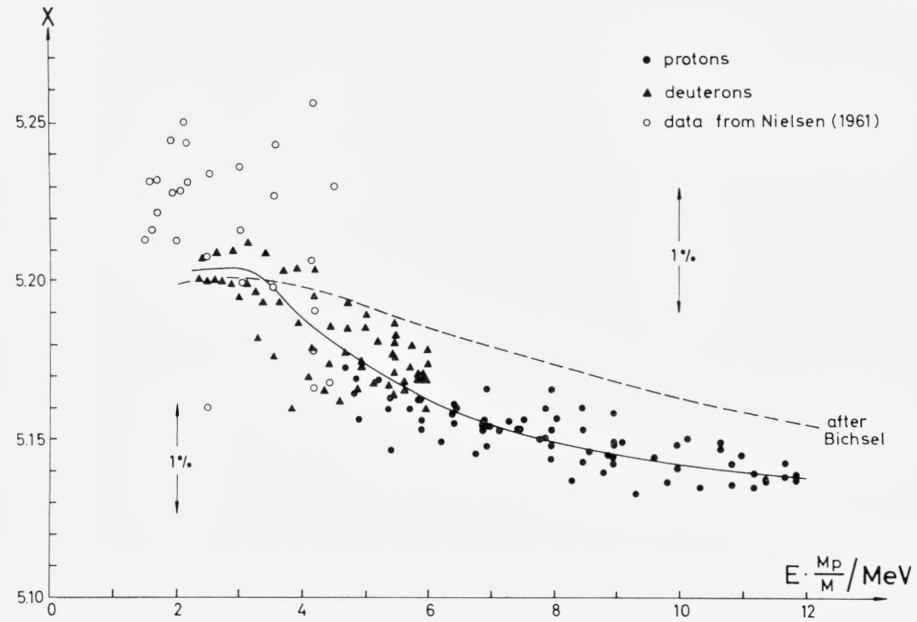

Figure 4. Measured stopping powers for aluminium in reduced variables defined by eq. (4.5). The height of the arrows indicates the change in X caused by a 1 % change in dE/dx. Open circles are measurements by Nielsen (1961) and the broken line tabulated values by Bichsel (1963 b). The full line is fitted to our experimental points by eye. $\frac{M_p}{M}$ = ratio between proton mass and mass of incident particle.

of each other (part II. B), and, in comparing, the combined uncertainty of the two calibrations has to be taken into account. The deviation is found not to be significant. It is, furthermore, certainly not due to crystallographic effects (part III) as this would introduce errors of the opposite sign.

There does not exist much other experimental information in this energy range with which it is possible to compare our results. The only relevant measurements are those of Nielsen (1961). Her points are shown as open circles. The results agree within her accuracy. It is also possible to compare our results with the tabulated values given by Bichsel (1963b). They are obtained by fitting the total amount of available data for aluminium, up to that time, to the expression (4.1) – including shell corrections. The fit is claimed to be good to 1 %, and the agreement is seen to be better than that. A very extensive table has also recently been published by Barkas and Berger (1964). The overall agreement with these tables is only good to about 2 %. Within the energies contained in fig. 4, the X-values computed

TABLE 2. Smoothed values of measured stopping powers for protons in aluminium obtained from the full line in fig. 4.
Experimental standard error ± 0.3 %

Energy MeV	$-dE/dx$ keV/mg cm^{-2}	Energy MeV	$-dE/dx$ keV/mg cm^{-2}
2.25	101.92	5.75	51.93
2.50	94.68	6.00	50.31
2.75	88.52	6.50	47.38
3.00	83.19	7.00	44.81
3.25	78.56	7.50	42.52
3.50	74.51	8.00	40.47
3.75	70.94	8.50	38.64
4.00	67.76	9.00	36.97
4.25	64.85	9.50	35.46
4.50	62.21	10.00	34.08
4.75	59.80	10.50	32.82
5.00	57.59	11.00	31.66
5.25	55.56	11.50	30.58
5.50	53.68	12.00	29.58

from their tables show such large fluctuations that they could not be contained in the figure.

We conclude that the accuracy of the tabulated data is within 0.3 %, and that the data agree with existing stopping power and range results within their estimated errors.

Acknowledgment

Special thanks are due to the Niels Bohr Institute, the University of Copenhagen, for letting us use a beam tube at the tandem accelerator. B. ELBEK and M. OLESEN from this institution gave us much advice concerning problems connected with the use of the accelerator. B. BORDRUP, G. DALSGAARD and A. NORDSKOV NIELSEN built the mechanical and electrical equipment with great care. P. VAJDA joined the group during the measurements and has taken part in the evaluation of some of the data presented here. Great stimulation came from the continuous interest of professors O. KOFOED-HANSEN and J. LINDHARD.

Appendix A

Coulomb Scattering in the Foil

The projectiles will have a longer path than the foil thickness because they are Coulomb-scattered by the target atoms. All particles undergo many small-angle scatterings while passing through the foil causing the beam to be gradually spread out, and a few particles are scattered through large angles thus travelling very much longer paths in the foil.

To be able to treat these two cases separately, we define an angle Θ_1 given by

$$Nt \int_{\Theta_1}^{\pi} \sigma(\Theta) d\Theta = 1 \tag{A 1}$$

where $\sigma(\Theta)$ is the differential Rutherford scattering cross section, i.e. Θ_1 is defined in such a way that particles passing through the foil will, in the mean, be scattered once through an angle Θ_1 or greater. We obtain

$$\Theta_1^2 = Nt \frac{\pi e^4 Z^2}{E^2} \tag{A 2}$$

by assuming $\Theta_1 \ll 1$ and substituting Z for $Z+1$. Scattering through angles smaller than Θ_1 is treated using multiple scattering theory and scattering through angles greater than Θ_1 by use of the Rutherford cross section.

If the beam has a mean square angular deviation Θ^2 from the normal, the relative correction to the energy loss will be

$$\frac{\delta(\Delta E)}{\Delta E} = \frac{\langle \Theta^2 \rangle}{2} \qquad \Theta^2 \ll 1. \tag{A 3}$$

Bethe and Ashkin (1953, p. 285) calculate Θ^2 to be

$$\langle \Theta \rangle^2 = \Theta_1^2 \ln \frac{\Theta_1^2}{\Theta_{\min}^2} \tag{A 4}$$

where $\Theta_{\min}$ is a minimum scattering angle given by the screening of the Coulomb interaction. This yields

$$\frac{\delta(\Delta E)_{\text{m.s.}}}{\Delta E} \simeq \frac{\langle \Theta^2 \rangle}{4} = \Theta_1^2 \cdot f\left(\frac{Z^{2/3} A}{t}\right) \tag{A 5}$$

provided $\langle\Theta^2\rangle \gg \Theta_1^2 \gg \Theta_{\min}^2$. f varies from 1.8 to 2.2 for all materials and thicknesses of interest to us.

To calculate the single-scattering correction the following model is assumed. The particles penetrate the foil with a constant energy E_0 to the point, where they are scattered. From this point they are assumed to lose energy at a rate given by the relation $R = c_2 \cdot E^2$ where R is the range of a particle with energy E and c_2 is an energy-independent constant, depending on projectile and target. This is a fairly good approximation corresponding to $dE/dx \propto 1/E$. The constant c_2 is eliminated from the final result.

We first calculate the energy of particles scattered in a thin layer dx situated the distance x beneath the back of the foil, $E'(E_0, \Theta, x)$. The total energy of all particles scattered through angles greater than Θ_1 leaving the foil will then be

$$E'(E_0, x)dx = dx \int_{\Theta_1}^{\pi} E'(E_0, \Theta, x)\sigma(\Theta)d\Theta. \tag{A 6}$$

If the particles were not scattered, they would leave the foil with energy $E(E_0, x)$, and the correction is

$$\delta_{\text{s.s.}}(E_0) = \int_0^t [E(E_0,x) - E'(E_0,x)]dx. \tag{A 7}$$

Performing the integration (A 6) we find

$$\left.\begin{aligned} E'_A(E_0,x) = &- c_1\sqrt{E_0^2 - x/c_2}\left[-\frac{4}{\Theta_1^2} + \frac{5}{3} + \frac{x/c_2}{E_0^2 - x/c_2}\right] - \\ &- \frac{c_1 x}{c_2\sqrt{E_0^2 - x/c_2}} \ln\left[\frac{8}{\Theta_1^2}\frac{c_2}{x}\left(E_0^2 - \frac{x}{c_2}\right)\right] \end{aligned}\right\} \tag{A 8}$$

and

$$\left.\begin{aligned} E'_C(E_0,x) = &\; c_1\sqrt{E_0^2 + \frac{x-t}{c_2}} + \\ &+ \frac{c_1(x-t)}{c_2\sqrt{E_0^2 + \frac{x-t}{c_2}}} \ln \frac{E_0^2 + \sqrt{E_0^4 - \left(\frac{x-t}{c_2}\right)^2}}{\frac{t-x}{c_2}} \end{aligned}\right\} \tag{A 9}$$

E_A refers to particles leaving the back of the foil, and E_C to those leaving the front. c_1 is the angularly independent factor in the Rutherford cross section. The integration (A 7) is carried through to second order in $\Delta E/E_0$. The relative single scattering correction is then found to be

$$\frac{\delta_{\text{s.s.}}}{\Delta E} = \frac{\Theta_1^2}{4}\left[2 + \ln\frac{8}{\Theta_1^2} + 2\ln\frac{E}{\Delta E}\right]. \tag{A 10}$$

Further details are given by ANDERSEN (1965).

Appendix B

Corrections Due to *x*-Rays and δ-Rays

Neglecting relativistic effects, (4.1) is written in the form

$$-\frac{dE}{dx} = \frac{4\pi e^4 Z^2}{mv^2}\frac{N_0}{A}\Sigma B_i \tag{B 1}$$

where

$$B_i = Z_i \ln\left(\frac{2mv^2}{I_i}\right). \tag{B 2}$$

The contributions have been split up for the different shells. Z_i is the number of electrons in the i^{th} shell, and I_i the ionization potential for this shell. Where necessary, the corrections due to WALSKE (1952, 1956) to (B 2) have been used. The fraction of the total energy loss due to the i^{th} shell is then

$$R_i = \frac{B_i}{\Sigma B_i}. \tag{B 3}$$

Some of this energy goes into kinetic energy of the expelled electron. If the fraction not doing so is f_i, the total energy stored in vacancies in the i^{th} shell will be $R_i \cdot f_i$. Due to the Auger effect only a fraction ω_i of this will appear as x-rays, and the total correction due to x-rays from the i^{th} shell and from a very thin foil is then

$$\frac{\delta_i}{\Delta E} = \omega_i f_i R_i \tag{B 4}$$

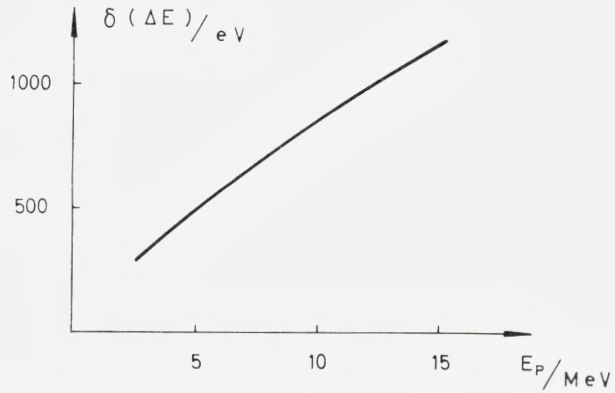

Figure 5. Energy being emitted as δ-rays from an aluminium foil traversed by a proton of energy E_p as calculated from (B 8).

This has a maximum for the K-shell of aluminium in our energy range of about $0.2\,\%$. For the L-shell in some of the heavier elements it might rise to $1.5\,\%$. Fortunately a good many of the x-rays are reabsorbed in the foil. If the absorption coefficient for a particular group of x-rays is μ, the self-absorption is a function only of the dimensionless quantity $a = \mu \cdot t$. The fraction escaping is

$$F(a) = \tfrac{1}{2}\left[\frac{1}{a} - \frac{e^{-a}}{a} + e^{-a} + a\mathrm{Ei}(-a)\right], \tag{B 5}$$

where $\mathrm{Ei}(a)$ is the Eire-function. This will usually reduce the correction by at least a factor of 3.

The δ-rays are energetic electrons emitted mainly in the forward direction. The electrons in the material are assumed to be free, and the energy distribution of the electrons is calculated by the Rutherford cross section, i.e. classically.

The probability that a single charged particle with velocity v will eject an electron with an energy in the interval Q to $Q + dQ$ from a slab with thickness dx is then

$$d\Sigma = \frac{N_0 Z}{A}\frac{2\pi e^4}{mv^2}\frac{dQ}{Q^2}\,dx = k \cdot \frac{dQ}{Q^2}\,dx. \tag{B 6}$$

These electrons are assumed to lose energy at a rate governed by a relation $R = c_2 \cdot E^2$ as in appendix A. If the slab is situated the distance x beneath the surface, the energy leaving the surface from this slab will be

$$E(x)dx = k \cdot dx \int_{\sqrt{T^2 + \frac{x}{c_2}\sqrt{\frac{T_m}{T}}}}^{T_m} \frac{1}{Q^2} \sqrt{Q^2 - \frac{x}{c_2}\sqrt{\frac{T_m}{Q}}}\, dQ \qquad \text{(B 7)}$$

where T_m is the maximum possible energy transfer. The total correction is then

$$\delta(E) = \int_0^{T_m} E(x)dx = \frac{N_0 Z}{A} \cdot c_2 \cdot \frac{\pi e^4 M}{m E_0} f(E) \qquad \text{(B 8)}$$

where $f(E)$ is a function only dependent on E, which has been found by numerical integration. The result for aluminium is shown in fig. 5.

Physics Department
Atomic Energy Commission
Research Establishment Risö
Roskilde, Denmark

A. F. Garfinkel
now at University of Wisconsin,
Madison, Wisconsin

References

H. H. Andersen (1965). A Low-Temperature Technique for Measurement of Heavy Particle Stopping Powers of Metals. Risø Report No. 93.

W. H. Barkas and M. J. Berger (1964). Tables of Energy Losses and Ranges of Heavy Charged Particles, in Studies in Penetration of Charged Particles in Matter. Publication 1133. National Academy of Science, Washington D.C.

H. A. Bethe and J. Ashkin (1953). Passage of Radiations through Matter, in E. Segre (edt.), Experimental Nuclear Physics, Wiley, N.Y.

H. Bichsel (1958). Experimental Range of Protons in Al. Phys. Rev. **112**, 1089.

H. Bichsel (1961 and 1963 a). Higher Shell Corrections in Stopping Power, and Appendix. Linear Accelerator Group. University of Southern California. Technical Report TR-3. (Unpublished).

H. Bichsel (1963 b). Passage of Charged Particles through Matter. American Institute of Physics Handbook. Second Edt. McGraw-Hill, N.Y.

H. Bichsel (1964). A Critical Review of Experimental Stopping Power and Range Data, in Studies in Penetration of Charged Particles in Matter. Publication 1133. National Academy of Science. Washington D.C.

H. Bichsel, W. Mozley and W. A. Aron (1957), Range of 6- to 18-MeV Protons in Be, Al, Cu, Ag and Au. Phys. Rev. **105**, 1788.

S. Datz, T. S. Noggle and C. D. Moak (1965), Anisotropic Energy Losses in a Face-Centered-Cubic Crystal for High-Energy ^{79}Br and ^{127}I Ions. Phys. Rev. Letters **15**, 254.

G. Dearnaley (1964), The Channeling of Ions through Silicon Detectors. IEEE Trans. Nucl. Sci. NS**11**, 249.

G. Dearnaley and A. R. Sattler (1964), Channeling of Ions through Single-Crystal Silicon Lattices. Bull. Am. Phys. Soc. **9**, 656.

G. Dearnaley and A. R. Sattler (1965), Channeling of Protons as a Function of Incident Angle in the ⟨110⟩ Plane in Silicon and Germanium. Bull. Am. Phys. Soc. **10**, 515.

C. Erginsoy, H. E. Wegner and W. M. Gibson (1964), Anisotropic Energy Loss of Light Particles of MeV Energies in Thin Silicon Single Crystals. Phys. Rev. Letters **13**, 530.

U. Fano (1963), Penetration of Protons, Alpha Particles, and Mesons. Ann. Rev. Nucl. Sci. **13**, 1.

F. Kalil, W. G. Stone, H. H. Hubbell and R. D. Birkhoff (1959), Stopping Power of Thin Aluminium Foils for 12 to 127 keV Electrons. ORNL 2731.

J. Lindhard (1964), Motion of Swift Charged Particles as Influenced by Strings of Atoms in Crystals. Phys. Letters **12**, 126.

J. Lindhard (1965), Influence of Crystal Lattice on Motion of Energetic Charged Particles. Mat. Fys. Medd. Dan. Vid. Selsk. **34**, No. 14.

L. P. Nielsen (1961), Energy Loss and Straggling of Protons and Deuterons. Mat. Fys. Medd. Dan. Vid. Selsk. **33**, No. 6.

M. C. Walske (1952), The Stopping Power of K-Electrons. Phys. Rev. **88**, 1283.

M. C. Walske (1957), Stopping Power of L-Electrons. Phys. Rev. **101**, 940.

P. L. Ziemer, R. M. Johnson and R. D. Birkhoff (1959), Measurement of Stopping Power of Copper by a Calorimetric Method. ORNL 2775.

Indleveret til Selskabet den 13. januar 1966.
Færdig fra trykkeriet den 25. juli 1966.